ACS NANO

www.acsnano.org

ARTICLE

Automating Blueprints for the Assembly of Colloidal Quasicrystal Clusters

Diogo E. P. Pinto, Petr Šulc, Francesco Sciortino, and John Russo*

Cite This: https://doi.org/10.1021/acsnano.4c10434

Read Online

ACCESS | Metrics & More | Article Recommendations | Supporting Information

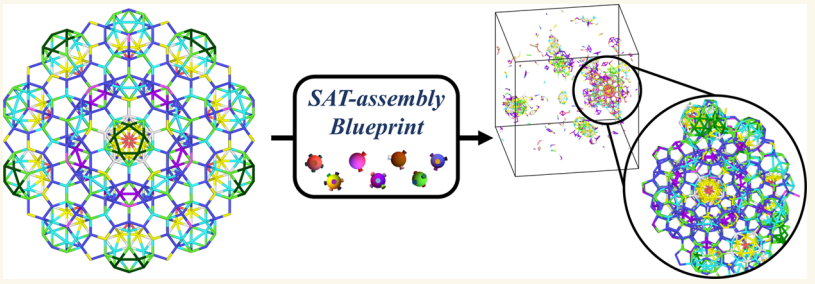

ABSTRACT: **One of the frontiers of nanotechnology is advancing beyond the periodic self-assembly of materials. Icosahedral quasicrystals, aperiodic in all directions, represent one of the most challenging targets that has yet to be experimentally realized at the colloidal scale. Previous attempts have required meticulous human-designed building blocks and often resulted in interactions beyond the current experimental capabilities. In this work, we introduce a framework for generating experimentally accessible designs that self-assemble into quasicrystalline arrangements. We present a design for icosahedral deoxyribonucleic acid (DNA) origami building blocks and demonstrate, through molecular simulations, their successful assembly into a target quasicrystalline structure. Our results highlight the feasibility of using automated design protocols to achieve complex quasicrystalline patterns, with applications in material science and nanotechnology.**

KEYWORDS: *self-assembly, quasicrystals, DNA origami, inverse design, patchy particles*

INTRODUCTION

One of the greatest achievements of nanotechnology is the self-assembly of crystalline structures with tailored properties, such as photonic crystals with omnidirectional band gaps.[1−5] The task of creating building blocks for crystal assembly is considerably facilitated by translational symmetry, which allows for targeting only a small number of particles (the unit cell) to direct the assembly pathway.[6,7] The biggest challenge encountered in crystal assembly is the need to select one and only one of the possible polymorphs (competing structures) as well as to avoid kinetic traps that arise from the bonding degeneracy of the building blocks.[8] Several approaches have been proposed to tackle these difficulties, from geometric design[9,10] to optimization methods.[11−13]

The problems faced in self-assembly become considerably more challenging when the target structures are aperiodic (as in quasicrystals) or when the unit cell becomes arbitrarily large (as in quasicrystal approximants, which have short-range quasicrystalline orientational order but long-range periodicity).[14−17] Over the years, multiple theoretical approaches have been proposed. In a more mathematically grounded approach, the structure of a quasicrystal can be conceptualized as a space-filling tiling of two or more different types of "unit cells" (or simply tiles).[18] The question then becomes how can one grow a minimal seed of tiles? Particularly, this is important since the correct tile to place at certain surface sites on the expanding cluster may rely on decisions made in far-off regions.[19] Naively, one could think that long-range interactions are necessary, but previous work has shown that local rules can be enough to nucleate and grow perfect (or with minimal defects) quasicrystals.[20,21] These usually take the form of matching rules between tiles, where the different types of tiles can only attach to each other along specific edges and relative orientations.[22] This can also be supplemented with forcing rules, where specific tiles are prioritized depending on local configurations of the surface environment.[23] Other approaches, grounded in colloidal physics, have focused on directional

Received: August 1, 2024
Revised: December 5, 2024
Accepted: December 11, 2024

interactions that enforce quasicrystalline orientational symmetry between simple building blocks. These interactions have either an entropic origin,[24] when controlled by particle shape, or an energetic origin, when controlled by selective bonds.[25] Recently, experimental realizations of deoxyribonucleic acid (DNA)-coated nanoparticles have successfully assembled the dodecagonal quasicrystal, which has 12-fold symmetry along one of its planes and is periodic along the perpendicular axis.[26] Other approaches have also achieved successful assemblies at the microscale, particularly in two dimensions (2D).[27]

One of the unmet goals is the laboratory realization of a fully aperiodic colloidal structure in three-dimensional (3D), such as the icosahedral quasicrystal. An important theoretical milestone in this direction was achieved by Noya and collaborators,[25] who designed a patchy particle model capable of assembling the icosahedral quasicrystal. The work utilized torsional interactions on top of colored patch specificity to nucleate the correct structure. Lee and Glotzer[28] were able to obtain 5-fold and icosahedral twinned clusters with purely repulsive interactions, utilizing the concept of entropic bonds as a way to drive hard core particles to assemble into specific structures, including quasicrystals.[24,29] In this case, the assembly is completely driven by entropy but requires particles to have specific shapes to properly form the patterns seen in the quasicrystals, and the high-density requirement for the assembly to be driven by entropy is still prohibitive for many applications. Recently, it has been shown that a system of hard spheres with two characteristic sizes in 2D is able to nucleate a quasicrystalline structure due to the high configurational entropy of the quasicrystal.[30] Moreover, these structures are able to accommodate a significant number of defects and still show the intended symmetries. This is observed due to the preference of the system to assemble the geometrical patterns that characterize the quasicrystal (square and triangles).

Here, we propose a solution derived from the SAT-assembly framework for the self-assembly of the icosahedral quasicrystal and its approximants. SAT is an automated strategy that converts the assembly problem into a Boolean Satisfiability Problem, which also allows for the suppression of competing structure formation.[31] Our design leverages existing building blocks, recently employed in the lab to assemble the pyrochlore lattice.[2] These building blocks consist of icosahedral DNA origami[32−36] with single-stranded overhangs. The nucleotide sequence of the overhangs encodes the specificity of the interaction, with bonds forming only when complementary strands on different icosahedral origami come together. This design relies exclusively on bond specificity and eliminates the need for additional interactions, such as torsional interactions, which are more difficult to engineer in DNA origami. This complexity increases when numerous interacting sites require precise torsional modulation to maintain specific angles between particles, as presented in the approach described in ref 25. As we alluded to above, the SAT-assembly method also allows us to incorporate the avoidance of common competing structures, i.e., crystal structures that would otherwise form with a subset of the components, into the solution. After deriving the solution, we map it to a patchy particle model[7,37−41] and run molecular simulations to verify that it correctly assembles the target structure. Finally, we demonstrate how the solution can be implemented using icosahedral DNA origami, which is based on previously experimentally realized designs.[2,42]

RESULTS AND DISCUSSION

SAT-Assembly for Quasicrystals. We approximate the icosahedral DNA origami by a patchy particle, where each patch corresponds to a DNA overhang. If we consider that each DNA sequence corresponds to a patch color, then the inverse design problem becomes a coloring problem. This can be approached by finding the number of colors, the way these are distributed through the patches, and the color interaction matrix such that it only assembles the target quasicrystal. For simple structures such a process can be done by hand, but as the complexity of the structure increases, so does the difficulty of the problem. Here, we use the previously developed SAT-assembly algorithm[31] to solve this task.

The SAT-assembly framework has so far been applied to crystals and finite-size structure with the same local environment, i.e., with the same geometry of the building block.[31,43−45] Here, we extend the framework to handle many local environments, such as those found in quasicrystals and their approximants. This allowed us to automatically generate blueprints for their assembly. SAT-assembly translates the self-assembly problem into a coloring problem, where the directional interaction of the building blocks is encoded in patches (attractive spots on the surface) and the specificity in their coloring. Each building block is distinguished not only by the geometrical arrangements of the patches but also by their coloring. In the following, the number of species—which corresponds to the number of unique building blocks—is indicated with N_p and the total number of colors with N_c.

The resulting SAT algorithm goes through the following steps:

i) Define the interparticle bonds in the target structure and assign to each particle a unique local environment (based on the topology of the bonding pattern). Nearest neighbor particles, defined as particles with a relative distance smaller than a cutoff threshold that includes the first three peaks of the radial distribution function, are considered bonded.

ii) Generate Boolean clauses that enforce the topology of the target structure and the exclusion of competing structures. The SAT clauses (ii) that enforce the topology are described in detail in the Supporting Information.

iii) Choose how many species N_p (i.e., different building blocks) to use for each environment, and the total number of colors N_c. The minimum value of N_p and N_c are such that the SAT problem is satisfiable; increasing their number increases the constraints on the self-assembly pathway but slows down its kinetics and is more challenging to realize experimentally. The right choice is usually a balance of these factors.

iv) Use SAT-solvers[46] to find a solution that consists of a coloring interaction table, the patch coloring of each species, and their position in the target structure. SAT-solvers are able to efficiently solve millions of clauses with millions of different boolean variables which is the typical range of the problems addressed here.

v) Run molecular simulations with the discovered design to assess its ability to reach the target structure. We run Monte Carlo simulations (v) with the Kern-Frenkel potential,[47,48] which is a minimal model still able to reproduce the self-assembly behavior of DNA origami with single-stranded overhangs.[2] Simulations are essen-

https://doi.org/10.1021/acsnano.4c10434
ACS Nano XXXX, XXX, XXX−XXX

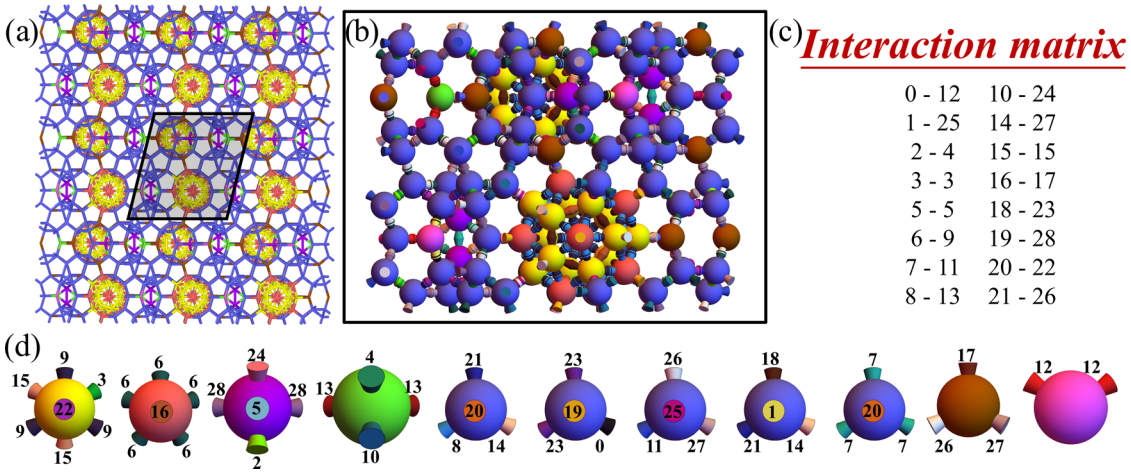

Figure 1. Schematic representation of the target structure and building blocks for the self-assembly of an icosahedral quasicrystal approximant. (a) Target structure used, the 3/2 icosahedral quasicrystal approximant, with only the bonds between the particles drawn. Each color represents an environment, where patch geometry is different. (b) Schematic representation of the unit cell with 284 particles and the respective colored patches corresponding to the 11 species and 29 colors design. (c, d) Details of the design used, particularly the different patch species and the corresponding interaction matrix between the patch colors. In this case, six of the species correspond to unique environments while the remainder five species correspond to the same 4-patch environment (blue).

tial to check whether the proposed design assembles into the desired structure.

vi) Simulations that do not form the target structure can be divided into two categories: in the first group, the self-assembly has been hindered by a competing structure; in the second, the kinetics of aggregation of the designs has favored amorphous aggregates. Within SAT-assembly the first problem can be avoided by including additional Boolean clauses which forbid the formation of the competing topology (going back to step ii). The second problem can be overcome by finding a new solution with an increased number of colors (going back to step iii). The ability to explicitly exclude the formation of competing structures is one of the main advantages of the SAT-assembly framework.

Icosahedral Quasicrystal Approximant. Quasicrystal approximants are periodic structures that exhibit properties similar to those of ideal quasicrystals. For example, an approximant produces a diffraction pattern resembling that of the ideal structure.[14] These structures can be generated using the cut-and-project method on a 6D hypercube,[49] which separates the higher-dimensional space into two orthogonal subspaces: the perpendicular and physical spaces. Following previous work,[25] we chose the B-type of the icosahedral quasicrysal as a starting point. In this approach, the cut is achieved by projecting a 6D body-centered hypercubic lattice onto the perpendicular space and excluding points outside a dodecahedral occupation domain. The choice of occupation domain determines the quasicrystal's point group symmetry. The subset of points within this domain is then projected back from 6D onto the physical plane, providing the particle positions for the ideal quasicrystal. The values used in the initial cut dictate the structure projected onto the physical space. If an irrational cut, such as the golden ratio, is used, then the ideal quasicrystal is generated. Alternatively, using two successive Fibonacci sequence numbers q/p produces a periodic q/p approximant. Figure 1a shows a section of the 3/2 icosahedral quasicrystal approximant, generated from the cut-and-project method, oriented along the pseudo-5-fold symmetry axis. Particles are considered to be bonded if their relative distance is smaller than 1.7 in the representation obtained from the cut-and-project method. This cutoff value separates first and second neighbors. We use this to define the patch geometries which can be organized into 7 unique environments (Figure 1d).

In the simulations, we consider a system composed of N patchy particles in a cubic box of length L. Each particle is characterized by a hard core of radius σ and $N_{patches}$ patches located on its surface, and it interacts with other particles according to the Kern-Frenkel potential.[47,48] Previous work has established that this modeling approach is a reasonable approximation of DNA origami systems.[39,40] Moreover, it has the advantage of being less computationally demanding, which makes the simulation of nucleation events feasible. In Figure 1b, we show a schematic representation of the unit cell of the 3/2 icosahedral quasicrystal approximant where each particle is given a color corresponding to their environment, and the different environment patch geometries are shown. The results shown below were obtained via Monte Carlo simulations using aggregation-biased moves.[50] More details regarding the simulation details can be found in the SI.

We consider that each patch can have a given color x_c between $0 \leq x_c < N_c$, where N_c is the total number of distinct colors. These colors can be distributed onto the patches in specific arrangements, and each unique sequence can be considered a particle species x_p, thus $1 \leq x_p \leq N_p$, where N_p is the total number of distinct species. SAT is then used to find if a given combination of N_p and N_c can satisfy the target structure, e.g., if it satisfies all of the topological constraints, and a solution/design is calculated which can be used to prepare the composition of the system. In the SI, we go into more detail on the different constraints (clauses) used for SAT. The particles shown in Figure 1c,d result from a design with 11 species and 29 colors. The 11 species corresponds to at least one of each environment plus other possible color variations for each. In this design, the blue 4-patch environment represents five of the species with different patch color arrangements, while the remainder six species correspond to unique environments with different patch geometries.

https://doi.org/10.1021/acsnano.4c10434
ACS Nano XXXX, XXX, XXX−XXX

Through the SAT formulation, we can recursively generate an array of different colored designs with different color arrangements. Moreover, we can constrain these designs to exclude specific competing structures. Previous works have noted that similar patch geometries can nucleate the *BC*8 crystal which directly competes with the icosahedral quasicrystal,[25] thus requiring torsional interactions to properly assemble the target structure. In our framework, we eliminate this minimum by constraining the patchy particle design to not satisfy the topology of the *BC*8 crystal unit cell (see the SI). The SAT algorithm guarantees that the patchy particle design shown in Figure 1c,d with 11 species and 29 colors does not satisfy the *BC*8 crystal topology.

For the following results, we have fixed the total number of species to 11, which corresponds to the distribution of environments shown in Figure 1d. Moreover, we also fix the species of each particle in the topology of the structure. Due to the high degree of complexity in the topology of the quasicrystal approximant, fixing these variables aids the SAT-solver in reaching a solution in reasonable time. To reach this value of species we have considered the bonded neighbors of each particle and kept only the unique arrangements of bonds between environments which cannot be obtained from simple rigid-body rotations of the particles. Then, through SAT, we can use different values for the total number of colors and create a pool of designs (patch color arrangements and colors interaction matrix) that can be tested for assembly. Figure 2 shows the results for nine different designs, going from 21 to 29 colors, where we have seeded one unit cell of the 3/2 icosahedral quasicrystal approximant (which contains 284 particles) in a cubic box with a total of $N = 2840$ particles. We run simulations at $T = 0.09$ (with the energy of the attractive interaction set to $\epsilon/k_B = 1$) and $\rho = 0.05$ (with the diameter of the individual particles set to $\sigma = 1$) to minimize the nucleation of other structures while allowing the seed to grow. We keep the same ratio of species as the one of the unit cell. We find that the size of the largest cluster increases with the total number of colors, while the total number of clusters decreases. Here, we only take into account the clusters larger than 82 particles, since that is the minimum number of particles to form the 32-particle icosahedral inner shell with the first layer around it containing 50 particles. Our simulations suggest that the unit cell starts growing from these structures. Given these results, we have chosen the 11 species and 29 colors design (Figure 1) to directly nucleate the target structure. For direct nucleation simulations, we randomly distribute $N = 5680$ particles in a cubic box with the same species ratio as the unit cell. In Figure 2b, we present a cluster that nucleated for $T = 0.096$ and $\rho = 0.1$, and has grown up to $N = 2221$ particles. We represent only the bonds between the particles and the cluster oriented along the pseudo-5-fold symmetry axis, clearly showing the intended symmetry. We have further calculated the diffraction pattern along this axis (Figure 2c) which highlights the 10 peaks corresponding to the pseudo-5-fold symmetry, thus confirming that the correct structure has nucleated.

Ideal Icosahedral Quasicrystal. Through the cut-and-project method, one can project onto physical space the ideal icosahedral quasicrystal by using only irrational cuts on the 6D hypercubic body-centered lattice. Unlike the previous structure, this one is aperiodic and shows 5-, 3-, and 2-fold symmetry. Figure 3 shows a schematic of a portion of the ideal icosahedral quasicrystal (1538 particles) where we have

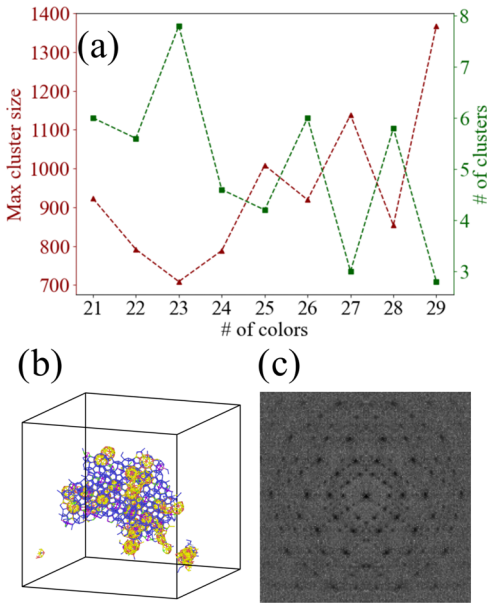

Figure 2. Seeding and direct nucleation of the icosahedral quasicrystal approximant. (a) Results for the icosahedral quasicrystal approximant, where the structure is seeded using a single unit cell of 284 particles at the center of the simulation box. The system is simulated for $\rho = 0.05$ and $T = 0.09$, and $\Delta t = 2 \cdot 10^7$. We simulate this system using nine different colored designs and show how the maximum cluster size and the total number of clusters change as a function of the total number of colors. The simulation box contains $N = 2680$ (including the initial seed) particles and we averaged over 5 different samples. (b) Cluster formed from a direct nucleation trajectory where only the bonds between particles are drawn. The direct nucleation simulation was done for $T = 0.096$, $\rho = 0.1$, $N = 5680$, and $\Delta t = 2 \cdot 10^8$. The cluster presented has size $N = 2221$ and is oriented along the pseudo-5-fold symmetry axis. (c) The corresponding diffraction pattern along this axis.

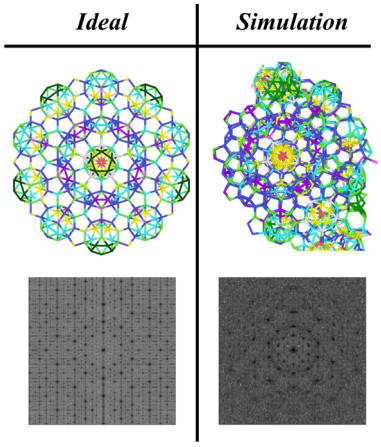

Figure 3. Direct nucleation of the ideal icosahedral quasicrystal. On the left is shown a portion of the ideal quasicrystal containing $N = 1538$ points which is used in the SAT framework to create the patchy particle designs for simulation. On the right is the simulated cluster obtained from direct nucleation simulations with $N = 1538$, $T = 0.0875$, $\rho = 0.05$, and for $\Delta t = 10^9$. Both clusters are oriented along the 5-fold symmetry axis, and the respective diffraction patterns are shown in the bottom panels.

connected the bonded particles. We have oriented the structure along the 5-fold symmetry axis and present the

https://doi.org/10.1021/acsnano.4c10434
ACS Nano XXXX, XXX, XXX−XXX

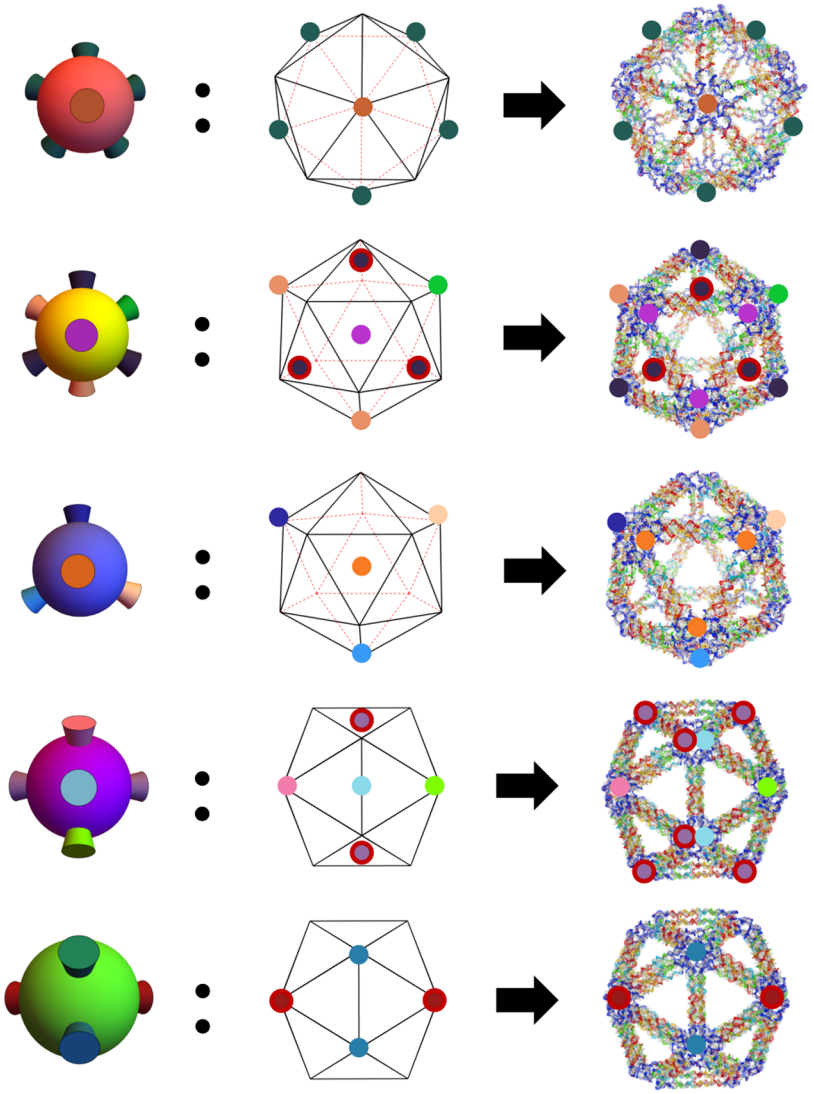

Figure 4. Schematic representation of the proposed realization of this system through icosahedral DNA origami. Each patchy particle environment corresponds to a given icosahedral DNA origami with patches on selected vertices. For each environment, we present a mapping onto the icosahedron and the respective DNA origami. The red dashed lines on the icosahedron correspond to the back faces, and the patch circles highlighted in red are located at the back of the origami with the rest being at the front. For two of the patchy particles used, all patches can be mapped directly to the vertices of the icosahedron (top and bottom environments). For the remaining three, we apply a mapping where a patch located on a face of the icosahedron is split into three identical patches at the nearest vertices while a patch on an edge is divided between the two closest vertices. This mapping guarantees correct alignment of the icosahedral DNA origami, which we previously used for experimental realizations of DNA lattice assemblies.[2]

diffraction pattern along this axis. The total number of unique environments is now 12 (SI). These include the ones shown in Figure 1d and some subsets of these with fewer patches. For example, one of the new environments corresponds to the 7-patch yellow particle in Figure 1d (first from the left) without one of the patches numbered 15.

For this structure, we used SAT to calculate patchy particle designs that satisfy the topology of the quasicrystal, which includes all 12 environments. The minimum number of particles for this condition is around $N = 1538$. We still keep the constraint that the designs should not satisfy the topology of the *BC*8 crystal unit cell. In this structure, the different environments bond between each other in 28 unique ways, and thus, we fix the total number of species to this value. By following a similar procedure as in the previous structure one can optimize the design for direct nucleation, which in this case corresponds to a 28 species and 27 colors design (details of the design can be found in the SI). We further introduce a two-step protocol for direct nucleation of this structure, where we start the simulations at a higher temperature (around $T = 0.12$) to form only the 32-particle icosahedral inner shell and then instantly quench to a lower temperature ($T = 0.0875$) to grow the structure. The icosahedral inner shell is able to form first since it includes the species with the most patches (7 and 6, respectively), leading to a higher bonding probability relative to the others. We have found that forming the initial 32-particle cluster significantly helps the self-assembly of the rest of the structure. We also note that we were not able to form this structure from the liquid, as it only consistently grew at lower densities ($\rho \leq 0.1$) from the gas phase. Figure 3 shows one of the clusters that formed in simulations with $\rho = 0.05$ oriented along the 5-fold symmetry axis. The diffraction pattern below is calculated along this axis and confirms the intended symmetry.

https://doi.org/10.1021/acsnano.4c10434
ACS Nano XXXX, XXX, XXX−XXX

To analyze the quasicrystallinity of our assembled structures, we do the reverse process of the cut-and-project method that was used to generate the ideal IQC. This "lifting" method maps every particle position onto a lattice point in 6D space. This can be achieved because the 6D interlattice vectors corresponding to each of the possible bond directions in the ideal IQC are known. Thus, by iterating through the bond network all particles can be "lifted" (more details in the SI). The phason strain in the assembled structure can then be calculated by examining the slope of the average distance between the "lifted" particles, projected onto a perpendicular space, as a function of their distance in the physical (parallel) space. In the SI, we show that the phason strain is negligible for the structure that targets the ideal IQC and compare it to the finite phason strain observed for the 3/2 approximant case. This result highlights the periodicity of the self-assembled structure. Lastly, one can also calculate the number of phason defects by projecting the "lifted" lattice points onto the perpendicular space and checking how many fall outside the acceptance domain. For the assembled structure shown in Figure 3, we observe a very small number of phason defects (less than 5%) suggesting that this structure is very similar to the targeted ideal IQC. This small difference can be attributed to local defects present in the structure that are formed during the self-assembly process. Dislocations can lead to ambiguity in the lifting process, but we observe no such case in our simulations.

Since our SAT approach only biases a local structure (subset) of the entire quasicrystal, it is not guaranteed that an assembled cluster can keep growing after reaching the respective subset size due to the structure being aperiodic. To assemble larger structures for the ideal quasicrystal, one needs to fully re-SAT a larger subset. It is also relevant to note that different projections of the IQC (from the cut-and-project method) could lead to similar local arrangements of particles, but yield a different global structure. To tackle this, it is ideal to SAT the largest cluster possible and assess if the assembled structures have a negligible phasing strain and a low number of phason defects. Our results provide strong support that this is the case for the structure in Figure 3.

Mapping onto Icosahedral Units. Recently, patchy particle models have proven highly effective as coarse-grained approaches for studying the assembly of DNA origami.[2] The quasicrystal designs proposed in the previous sections can be mapped onto an icosahedron, allowing for functionalization with single DNA strands at its vertices. Figure 4 shows a possible mapping of the different patch geometries onto icosahedron DNA origami. In this mapping, we chose to retain the patch positions that align with the icosahedron's vertices, while redistributing those that fall on its faces or edges. To achieve this, patches located on the icosahedron's faces were replaced by three new patches at the nearest vertices, while those on the edges were replaced by two new patches at the closest vertices. This mapping guarantees proper orientation of the DNA origami wireframe for the assembly of the icosahedral quasicrystal.

CONCLUSIONS

In this work, we have proposed an automated method to generate patchy particle designs with colored interactions that can self-assemble the icosahedral quasicrystal and its approximants. We use a simple patchy particle model with attractive surface patches that are colored such that they bond only with the complementary color. This selective interaction can be described as a SAT problem and efficiently solved numerically to produce designs (patch color distribution and color−color interaction matrix) that target specific structures. One can then test the designs in coarse-grained simulations to understand their efficacy. We demonstrate how to use this strategy to self-assemble the 3/2 icosahedral quasicrystal approximant, which shows the pseudo-5-fold symmetry axis characteristic of this structure. We then expand this procedure to target the ideal quasicrystal by using a design that satisfies a portion of the structure. Through a 2-step temperature quench protocol, we are able to self-assemble this structure in simulations and highlight its 5-fold symmetry axis through the diffraction pattern. Moreover, we show that the assembled structure has negligible phason strain and a low number of phason defects. Lastly, we introduce a possible mapping of our patchy particle design onto a DNA origami icosahedron. By mapping patches that are positioned at the faces and edges to the closest vertices, we are able to propose a DNA origami that only requires DNA strands to be functionalized to the vertices. This guarantees the required orientational order of the icosahedral quasicrystal. Given this mapping and the simplicity of the patchy particle model used, we believe such designs are amenable to experiments as demonstrated for the case of pyrochlore lattice in recent work.[2]

Our results demonstrate that using only colored patch specificity is enough to nucleate these structures. Thus, even with a simple patch−patch interaction, the intended orientational symmetry can be propagated. Our method is also fully automated and can be arbitrarily constrained to fit the experimental requirements. For example, for all of the designs shown here, each color only interacts with one other. In the context of DNA origami, our simplification of the patchy particle interactions should allow for easier translation of the simulations into experiments.

In the context of quasicrystal tilings, it is possible to devise matching rules between the different tile types to grow a quasicrystalline structure from a seed.[20] These rules usually define how the tiles connect to each other, specifically in terms of relative positioning.[22] The key point is that these rules are local but still enforce global quasicrystalline symmetry.[19] In our case, a tile is represented by a group of bonded patchy particles. By using SAT to constrain the particle coloring, we are indirectly enforcing the matching rules in a portion of the quasicrystal. One can abstract this coloring problem and consider that the particles at the vertices of the respective tiles will bond only when the colors are complementary. Thus, the tiles themselves can be thought of as coloring units, which are also constrained through SAT, meaning that the matching rules must also be satisfied via SAT constraints. Since we only SAT a portion of the quasicrystal, it is possible that we do not capture all of the necessary complexity to enforce all matching rules. It is important to note that, due to experimental constraints,[2] additional considerations must be made. For example, we always require that each patch color interacts with only one other complementary color, which is not a typical constraint for matching rules.

During submission of this manuscript, we became aware of the recent work by Noya and Doye[51] who rationally designed a one-component patchy particle to self-assemble a face-centered icosahedral quasicrystal. The advantage of their solution is the simplicity of the building block, but it requires two energy scales. Our method instead suggests the use of multiple species

https://doi.org/10.1021/acsnano.4c10434
ACS Nano XXXX, XXX, XXX−XXX

in order to work with a single energy scale and additional experimental constraints, such as having orthogonal interactions (i.e., each color has only one complementary color and does not interact with other colors), which can be translated into DNA-sequences more easily.

METHODS

We consider a system composed of N patchy particles in a cubic box with a length of L. Particles are characterized by a hard core of diameter σ with $N_{patches}$ patches on its surface. The patches interact through the Kern-Frenkel potential:[47,48]

$$V\mathrm{pp}(\boldsymbol{r}_{ij}, \hat{\boldsymbol{r}}_{\alpha,i}, \hat{\boldsymbol{r}}_{\beta,j}) = V_{\mathrm{SW}}(r_{ij}) f(\boldsymbol{r}_{ij}, \hat{\boldsymbol{r}}_{\alpha,i}, \hat{\boldsymbol{r}}_{\beta,j}) \quad (1)$$

where i corresponds to a given particle and $\boldsymbol{r}_i$ its center of mass. Thus, $\boldsymbol{r}_{ij}$ is the distance between particles i and j. $\boldsymbol{r}_{\alpha,i}$ denotes the position of patch α of particle i. V_{SW} is an isotropic square well of range $\sigma + \delta_{\alpha,\beta}$ and depth $\varepsilon_{\alpha,\beta}$. The hat symbol indicates unit vectors, and f is the orientation-dependent modulation term that takes the form:

$$f(\boldsymbol{r}_{ij}, \hat{\boldsymbol{r}}_{\alpha,i}, \hat{\boldsymbol{r}}_{\beta,j}) = \begin{cases} 1 & \text{if } \begin{array}{l} \hat{\boldsymbol{r}}_{ij}\cdot\hat{\boldsymbol{r}}_{\alpha,i} > \cos\theta_{\alpha\beta}^{\max} \\ \hat{\boldsymbol{r}}_{ji}\cdot\hat{\boldsymbol{r}}_{\beta,j} > \cos\theta_{\alpha\beta}^{\max} \end{array} \\ 0 & \text{otherwise} \end{cases} \quad (2)$$

With this formulation, patches are represented by a cone starting from the center of mass of the particle and reaching $\sigma + \delta_{\alpha,\beta}$, while the width is controlled by $\theta_{\alpha\beta}^{\max}$. For simplicity, we consider the parameter range where it is only possible to form one bond per patch. In the following, σ provides the unit of length and $\varepsilon_{\alpha,\beta}$ the unit of energy. Temperature (T) is also expressed in units of $\varepsilon_{\alpha,\beta}$ and $k_B = 1$.

For the results, we considered Monte Carlo (MC) simulations with two possible moves, roto-translations and aggregation-volume-bias.[50] The first attempts simple rotation and translation of a random particle along a random (radial or angular) direction. The second attempts to move a random particle into the vicinity of another such that a bond is formed between the two. To not break ergodicity, the inverse move can also be performed, where a random bond between two particles is broken. We performed simulations in the NVT ensemble to explore the assembly of the desired structures. For the results shown, we considered $\delta_{\alpha,\beta} = 0.2$ and $\cos\theta_{\alpha\beta}^{\max} = 0.98$. The direct nucleation simulations start with particles randomly generated in the box with random orientations. The seeding simulations start with the seed placed at the center of the box and the rest of the particles randomly distributed, with a buffer space between the seed and the rest of the particles with sizes on the order of a single particle diameter.

The code implementing the SAT-assembly pipeline is available at: https://github.com/deppinto/PatchyParticles.

The homemade code to calculate the diffraction patterns makes use of the FFTW package[52] and can be found at: https://github.com/deppinto/PatchyParticles/IQC.

ASSOCIATED CONTENT

Supporting Information

The Supporting Information is available free of charge at https://pubs.acs.org/doi/10.1021/acsnano.4c10434.

Simulations and the SAT-assembly framework; information used in SAT to calculate the designs for quasicrystal assembly; more details regarding the simulations and self-assembly protocols; and "lifting" method (PDF)

AUTHOR INFORMATION

Corresponding Author

John Russo − *Dipartimento di Fisica, Sapienza Università di Roma, 00185 Rome, Italy;* orcid.org/0000-0002-6234-6344; Email: john.russo@uniroma1.it

Authors

Diogo E. P. Pinto − *Dipartimento di Fisica, Sapienza Università di Roma, 00185 Rome, Italy*

Petr Šulc − *School of Molecular Sciences and Center for Molecular Design and Biomimetics, The Biodesign Institute, Arizona State University, Tempe, Arizona 85281, United States; School of Natural Sciences, Department of Bioscience, Technical University Munich, 85748 Garching, Germany;* orcid.org/0000-0003-1565-6769

Francesco Sciortino − *Dipartimento di Fisica, Sapienza Università di Roma, 00185 Rome, Italy;* orcid.org/0000-0002-2418-2713

Complete contact information is available at: https://pubs.acs.org/10.1021/acsnano.4c10434

Notes

The authors declare no competing financial interest.

ACKNOWLEDGMENTS

D.E.P.P., J.R., and F.S. acknowledge partial support by ICSC−Centro Nazionale di Ricerca in High Performance Computing, Big Data and Quantum Computing, funded by European Union−NextGenerationEU, and the CINECA award under the ISCRA initiative, for the availability of high-performance computing resources and support. D.E.P.P. and F.S. acknowledge support from MIUR-PRIN Grant No. 2022JWAF7Y. Work by P.S. was supported by the U.S. Department of Energy (DOE), Office of Science, Basic Energy Sciences (BES) under Award Number DE-SC0025265. We thank Michael Matthies for help with visualization of DNA origami.

REFERENCES

(1) Posnjak, G.; Yin, X.; Butler, P.; Bienek, O.; Dass, M.; Lee, S.; Sharp, I. D.; Liedl, T. Diamond-lattice photonic crystals assembled from DNA origami. *Science* **2024**, *384*, 781−785.

(2) Liu, H.; Matthies, M.; Russo, J.; Rovigatti, L.; Narayanan, R. P.; Diep, T.; McKeen, D.; Gang, O.; Stephanopoulos, N.; Sciortino, F.; Yan, H.; Romano, F.; Šulc, P. Inverse design of a pyrochlore lattice of DNA origami through model-driven experiments. *Science* **2024**, *384*, 776−781.

(3) Macfarlane, R. J.; Lee, B.; Jones, M. R.; Harris, N.; Schatz, G. C.; Mirkin, C. A. Nanoparticle Superlattice Engineering with DNA. *Science* **2011**, *334*, 204−208.

(4) Jones, M. R.; Seeman, N. C.; Mirkin, C. A. Programmable materials and the nature of the DNA bond. *Science* **2015**, *347*, No. 1260901.

(5) Nykypanchuk, D.; Maye, M. M.; van der Lelie, D.; Gang, O. DNA-guided crystallization of colloidal nanoparticles. *Nature* **2008**, *451*, 549−552.

(6) Romano, F.; Sanz, E.; Sciortino, F. Crystallization of tetrahedral patchy particles in silico. *J. Chem. Phys.* **2011**, *134*, No. 174502.

(7) Wang, Y.; Wang, Y.; Breed, D. R.; Manoharan, V. N.; Feng, L.; Hollingsworth, A. D.; Weck, M.; Pine, D. J. Colloids with valence and specific directional bonding. *Nature* **2012**, *491*, 51−55.

(8) Whitelam, S.; Jack, R. L. The Statistical Mechanics of Dynamic Pathways to Self-Assembly. *Annu. Rev. Phys. Chem.* **2015**, *66*, 143−163.

(9) Videbæk, T. E.; Hayakawa, D.; Grason, G. M.; Hagan, M. F.; Fraden, S.; Rogers, W. B. Economical routes to size-specific assembly of self-closing structures. *Sci. Adv.* **2024**, *10*, No. eado5979.

(10) Flavell, W.; Neophytou, A.; Demetriadou, A.; Albrecht, T.; Chakrabarti, D. Programmed Self-Assembly of Single Colloidal Gyroids for Chiral Photonic Crystals. *Adv. Mater.* **2023**, *35*, No. 2211197.

(11) King, E. M.; Du, C. X.; Zhu, Q.-Z.; Schoenholz, S. S.; Brenner, M. P. Programming patchy particles for materials assembly design. *Proc. Natl. Acad. Sci. U.S.A.* **2024**, *121*, No. e2311891121.
(12) Coli, G. M.; Boattini, E.; Filion, L.; Dijkstra, M. Inverse design of soft materials via a deep learning–based evolutionary strategy. *Sci. Adv.* **2022**, *8*, No. eabj6731.
(13) Adorf, C. S.; Moore, T. C.; Melle, Y. J. U.; Glotzer, S. C. Analysis of Self-Assembly Pathways with Unsupervised Machine Learning Algorithms. *J. Phys. Chem. B* **2020**, *124*, 69–78. PMID: 31813215.
(14) Goldman, A. I.; Kelton, R. F. Quasicrystals and crystalline approximants. *Rev. Mod. Phys.* **1993**, *65*, 213–230.
(15) Baake, M. A Guide to Mathematical Quasicrystals. 1999, p. 9901014. https://arxiv.org/abs/math-ph/9901014. (accessed April 12, 2024).
(16) Bindi, L.; Steinhardt, P. J.; Yao, N.; Lu, P. J. Natural Quasicrystals. *Science* **2009**, *324*, 1306–1309.
(17) Nagao, K.; Inuzuka, T.; Nishimoto, K.; Edagawa, K. Experimental Observation of Quasicrystal Growth. *Phys. Rev. Lett.* **2015**, *115*, No. 075501.
(18) Socolar, J. E. S.; Steinhardt, P. J. Quasicrystals. II. Unit-cell configurations. *Phys. Rev. B* **1986**, *34*, 617–647.
(19) Katz, A. Matching Rules and Quasiperiodicity: the Octagonal Tilings. In *Beyond Quasicrystals*; Springer: Berlin, Heidelberg, 1995; pp 141–189.
(20) Ingersent, K.; Steinhardt, P. J. Matching rules and growth rules for pentagonal quasicrystal tilings. *Phys. Rev. Lett.* **1990**, *64*, 2034–2037.
(21) Kuczera, P.; Steurer, W. Cluster-Based Solidification and Growth Algorithm for Decagonal Quasicrystals. *Phys. Rev. Lett.* **2015**, *115*, No. 085502.
(22) Onoda, G. Y.; Steinhardt, P. J.; DiVincenzo, D. P.; Socolar, J. E. S. Growing Perfect Quasicrystals. *Phys. Rev. Lett.* **1988**, *60*, 2653–2656.
(23) Hann, C. T.; Socolar, J. E. S.; Steinhardt, P. J. Local growth of icosahedral quasicrystalline tilings. *Phys. Rev. B* **2016**, *94*, No. 014113.
(24) Engel, M.; Damasceno, P. F.; Phillips, C. L.; Glotzer, S. C. Computational self-assembly of a one-component icosahedral quasicrystal. *Nat. Mater.* **2015**, *14*, 109–116.
(25) Noya, E. G.; Wong, C. K.; Llombart, P.; Doye, J. P. How to design an icosahedral quasicrystal through directional bonding. *Nature* **2021**, *596*, 367–371.
(26) Zhou, W.; Lim, Y.; Lin, H.; Lee, S.; Li, Y.; Huang, Z.; Du, J. S.; Lee, B.; Wang, S.; Sánchez-Iglesias, A.; et al. Colloidal quasicrystals engineered with DNA. *Nat. Mater.* **2024**, *23*, 424–428.
(27) Plati, A.; Maire, R.; Fayen, E.; Boulogne, F.; Restagno, F.; Smallenburg, F.; Foffi, G. Quasi-crystalline order in vibrating granular matter. *Nat. Phys.* **2024**, *20*, 1–7.
(28) Lee, S.; Glotzer, S. C. Entropically engineered formation of fivefold and icosahedral twinned clusters of colloidal shapes. *Nat. Commun.* **2022**, *13*, No. 7362.
(29) Vo, T.; Glotzer, S. C. A theory of entropic bonding. *Proc. Natl. Acad. Sci. U.S.A.* **2022**, *119*, No. e2116414119.
(30) Fayen, E.; Filion, L.; Foffi, G.; Smallenburg, F. Quasicrystal of Binary Hard Spheres on a Plane Stabilized by Configurational Entropy. *Phys. Rev. Lett.* **2024**, *132*, No. 048202.
(31) Russo, J.; Romano, F.; Kroc, L.; Sciortino, F.; Rovigatti, L.; Šulc, P. SAT-assembly: a new approach for designing self-assembling systems. *J. Phys.:Condens. Matter* **2022**, *34*, 354002.
(32) Sigl, C.; Willner, E. M.; Engelen, W.; Kretzmann, J. A.; Sachenbacher, K.; Liedl, A.; Kolbe, F.; Wilsch, F.; Aghvami, S. A.; Protzer, U.; et al. Programmable icosahedral shell system for virus trapping. *Nat. Mater.* **2021**, *20*, 1281–1289.
(33) Mosayebi, M.; Shoemark, D. K.; Fletcher, J. M.; Sessions, R. B.; Linden, N.; Woolfson, D. N.; Liverpool, T. B. Beyond icosahedral symmetry in packings of proteins in spherical shells. *Proc. Natl. Acad. Sci. U.S.A.* **2017**, *114*, 9014–9019.
(34) Lee, J. G.; Kim, K. S.; Lee, J. Y.; Kim, D.-N. Predicting the Free-Form Shape of Structured DNA Assemblies from Their Lattice-Based Design Blueprint. *ACS Nano* **2022**, *16*, 4289–4297.
(35) Jun, H.; Wang, X.; Parsons, M. F.; Bricker, W. P.; John, T.; Li, S.; Jackson, S.; Chiu, W.; Bathe, M. Rapid prototyping of arbitrary 2D and 3D wireframe DNA origami. *Nucleic Acids Res.* **2021**, *49*, 10265–10274.
(36) Rothemund, P. W. K. Folding DNA to create nanoscale shapes and patterns. *Nature* **2006**, *440*, 297–302.
(37) Sacanna, S.; Pine, D. J. Shape-anisotropic colloids: Building blocks for complex assemblies. *Curr. Opin. Colloid Interface Sci.* **2011**, *16*, 96–105.
(38) Wang, Y.; Wang, Y.; Zheng, X.; Ducrot, É.; Yodh, J. S.; Weck, M.; Pine, D. J. Crystallization of DNA-coated colloids. *Nat. Commun.* **2015**, *6*, No. 7253.
(39) Rovigatti, L.; Russo, J.; Romano, F.; Matthies, M.; Kroc, L.; Šulc, P. A simple solution to the problem of self-assembling cubic diamond crystals. *Nanoscale* **2022**, *14*, 14268–14275.
(40) Ravaine, S.; Duguet, E. Synthesis and assembly of patchy particles: Recent progress and future prospects. *Curr. Opin. Colloid Interface Sci.* **2017**, *30*, 45–53.
(41) Pawar, A. B.; Kretzschmar, I. Fabrication, assembly, and application of patchy particles. *Macromol. Rapid Commun.* **2010**, *31*, 150–168.
(42) Zhang, J.; Xu, Y.; Huang, Y.; Sun, M.; Liu, S.; Wan, S.; Chen, H.; Yang, C.; Yang, Y.; Song, Y. Spatially Patterned Neutralizing Icosahedral DNA Nanocage for Efficient SARS-CoV-2 Blocking. *J. Am. Chem. Soc.* **2022**, *144*, 13146–13153.
(43) Bohlin, J.; Turberfield, A. J.; Louis, A. A.; Šulc, P. Designing the Self-Assembly of Arbitrary Shapes Using Minimal Complexity Building Blocks. *ACS Nano* **2023**, *17*, 5387–5398.
(44) Pinto, D. E. P.; Šulc, P.; Sciortino, F.; Russo, J. Design strategies for the self-assembly of polyhedral shells. *Proc. Natl. Acad. Sci. U.S.A.* **2023**, *120*, No. e2219458120.
(45) Romano, F.; Russo, J.; Kroc, L.; Šulc, P. Designing patchy interactions to self-assemble arbitrary structures. *Phys. Rev. Lett.* **2020**, *125*, No. 118003.
(46) Eén, N.; Biere, A. Effective preprocessing in SAT through variable and clause elimination. *Lect. Notes Comput. Sci.* **2005**, *3569*, 61–75.
(47) Bol, W. Monte Carlo simulations of fluid systems of waterlike molecules. *Mol. Phys.* **1982**, *45*, 605–616.
(48) Kern, N.; Frenkel, D. Fluid–fluid coexistence in colloidal systems with short-ranged strongly directional attraction. *J. Chem. Phys.* **2003**, *118*, 9882.
(49) Baake, M.; Grimm, U. *Aperiodic Order*, Encyclopedia of Mathematics and its Applications; Cambridge University Press, 2013.
(50) Rovigatti, L.; Russo, J.; Romano, F. How to Simulate Patchy Particles. *Eur. Phys. J. E* **2018**, *41*, 59.
(51) Noya, E. G.; Doye, J. P. K. A One-component Patchy-particle Icosahedral Quasicrystal; 2024, 2407.17212. arXiv. https://arxiv.org/abs/2407.17212. (accessed April 12, 2024).
(52) Frigo, M.; Johnson, S. G. The Design and Implementation of FFTW3. *Proc. IEEE* **2005**, *93* (2), 216–231.

https://doi.org/10.1021/acsnano.4c10434
ACS Nano XXXX, XXX, XXX–XXX